https://doi.org/10.5194/acp-2022-542
Preprint. Discussion started: 2 September 2022

Atmospheric Chemistry and Physics Discussions

Variations of the density of ambient black carbon retrieved by a new method: importance to CCN prediction

Jingye Ren[1, 2], Fang Zhang[2*], Lu Chen[1], Jieyao Liu[1]

[1]*College of Global Change and Earth System Science, Beijing Normal University, Beijing 100875, China*

[2]*School of Civil and Environmental Engineering, Harbin Institute of Technology (Shenzhen), 518055 Shenzhen, China*

***Correspondence to:* Fang Zhang (zhangfang2021@hit.edu.cn)**

https://doi.org/10.5194/acp-2022-542
Preprint. Discussion started: 2 September 2022

Atmospheric Chemistry and Physics Discussions

Abstract.

The effective density of black carbon (BC) is a crucial factor relevant to its morphology and mixing state that would add uncertainty in evaluating its climate effect. Here, we develop a new method to retrieve the effective density of ambient BC combining field observations with the Köhler theory. The uncertainty of the new retrieval method was evaluated within ±30 %, which is primarily caused by assumptions of the hygroscopic parameter of organics and the fraction of primary organic aerosols in non-hygroscopic or hygroscopic mode. Using the new method, we obtain that the ambient BC density during the campaign varies widely from 0.14 to 2.1 g cm^{-3}, with a campaign mean density of 1.11±0.54 g cm^{-3} for internally-mixed BC that accounts for 79±18 % of total BC particles. The retrieved values fall within the range of typical density of internally-mixed BC reported in the literatures. We further examined the sensitivity of cloud condensation nuclei (CCN) number concentrations (N_{CCN}) prediction to variations of BC density, showing an uncertainty of -28 %~11 % in calculating N_{CCN} at supersaturations of 0.2 % and 0.4 % by varying the BC density within the retrieved ranges. We also find that the N_{CCN} is more sensitive to the variations of BC density when it is <1.0 g cm^{-3}, illustrating a necessity of accounting for such effect closer to source regions where the BC particles are mostly freshly emitted. The CCN closure achieves when introducing the retrieved real-time BC density and mixing state. This study provides a unique way of utilizing field measurements to infer ambient BC density and highlights the importance of applying varying BC density values in

https://doi.org/10.5194/acp-2022-542
Preprint. Discussion started: 2 September 2022


Atmospheric Chemistry and Physics Discussions

models when predicting CCN and assessing its relevant climate effect.

1 Introduction

Black carbon (BC) aerosols, as the major absorber of solar radiation, play a vital role in energy budget and climate of the earth-atmosphere system by affecting the radiative forcing and cloud properties (Flanner et al., 2007; Ramanathan and Carmichael, 2008). The capability of light-absorbing induced by BC is related to its density and morphology (Zhang et al., 2008; Rissler et al., 2014), which can be modified after mixing with other atmospheric aerosol particles (Khalizov et al., 2009; Xue et al., 2009). Changes in its physicochemical properties would also regulate its ability to serve as cloud condensation nuclei (CCN) and further indirectly affect the radiative balance by affecting the clouds process (Yuan et al., 2008; Wang et al., 2011). Owing to the complex evolution of the mixing state, density and morphology of BC, the contribution of BC particles to CCN budgets is still not well understand.

BC particles, with diesel vehicles, industrial and residential coal combustion as major sources, are ubiquitous in urban environments (Bond et al., 2013; Dameto et al., 2017; Li et al., 2017; D. Liu et al., 2019). Typically, freshly generated BC exists in the form of chain aggregates. While after aging, the BC particles generally mix with other materials by condensation, coagulation, and other processes (Riemer et al., 2004; Zhang et al., 2008; Liu et al., 2013; Zhang et al., 2020). The structure of BC would be more compact with regular shapes (Pagels et al., 2009; Zhang et al., 2008; Wang et al., 2017), and the effective density of BC are changed accordingly with the reconstruction (H. Liu

https://doi.org/10.5194/acp-2022-542
Preprint. Discussion started: 2 September 2022


Atmospheric Chemistry and Physics Discussions

et al., 2019). The density and morphology of BC particles are closely related to its sources, mobility size after aging, coating thickness, coating material and its chemical composition (Zhang et al., 2008; Pagels et al., 2009; Peng et al., 2016; Zhang et al., 2022). A wide range of BC density has been reported in previous studies (Lide 1992; Mcmurry et al., 2002; Park et al., 2004; Kiselev et al., 2010). Recent field measurements have indicated that the average density of BC is ~1.2 g cm^{-3} in the ambient atmosphere (Zhang et al., 2016). Field measurements have also indicated that a fraction of externally mixed/uncoated BC exists (Clarke et al., 2004; Cheng et al., 2012; Chen et al., 2020) and even higher than that internal/ aged BC particles in the ambient atmosphere (Schwarz et al., 2008; Massoli et al., 2015). While, in climate models, the BC was generally assumed internally-mixed and treated to have a void-free spherical structure and a density value of 1.8 g cm^{-3} (Bond et al., 2013). This may lead to bias in estimating the climate effects driven by BC.

Previous study based on a case study show that when the aging degree of ambient particles is low, the BC density (~1.8 g cm^{-3}) under the spherical assumption will lead to the overestimation of particles hygroscopicity by 40-50 % and the overestimation can be explained almost 100 % by using the effective density of fresh BC (~0.45 g cm^{-3}) (Fan et al. 2020). This indicates the importance of using reasonable BC density values in the calculation of particle hygroscopicity. In addition, when estimating the CCN number concentration, a significant bias of –35 % ~ +20 % was found caused by the assumption of particle mixing state (Ren et al., 2018). However, these studies have not yet account for such impact of BC density and mixing state on CCN prediction due to

https://doi.org/10.5194/acp-2022-542
Preprint. Discussion started: 2 September 2022


Atmospheric Chemistry and Physics Discussions

lack of real time measurement data.

The mixing state and the density of BC particles are usually directly measured by several techniques, such as an integrated system of a volatility tandem differential mobility analyzer and a single particle soot photometer (VTDMA-SP2) (Zhang et al., 2016), or a differential mobility analyzer with a SP2 (DMA-SP2) (Olfert et al., 2007; Rissler et al., 2014; Wu et al., 2019), and a differential mobility analyzer–centrifugal particle analyzer–single-particle soot photometer (DMA–CPMA–SP2) system (H. Liu et al., 2019; Yu et al., 2020), etc. However, such techniques or measurements are not available in many previously conducted filed campaigns. In this study, we develop a novel method for retrieving the mixing state and effective density of ambient BC particles by combining field measured hygroscopic growth factor and aerosol chemical composition and Köhler theory (Petters and Kreidenweis, 2007). The uncertainty of the new retrieval method was evaluated. The retrieved results were also compared and validated with existing observations. In addition, the effect of BC density and mixing state on prediction of CCN number concentrations is further evaluated through a sensitivity and closure test by accounting for the retrieved real-time variations of BC density and mixing state.

2 Field measurements and methodology

2.1 Field measurements

Measurements in this study were conducted from 15 November to 14 December 2016 at a typical urban site of Beijing (39.97°N, 116.37°E, 49 m above sea level). The

https://doi.org/10.5194/acp-2022-542
Preprint. Discussion started: 2 September 2022


Atmospheric Chemistry and Physics Discussions

site locates at the Institute of Atmospheric Physics, Chinese Academy of Sciences, which is mainly influenced by the surrounding cooking, road traffic and residential coal burning emissions during the home heating periods (Sun et al., 2016). The detailed information about the sampling site was presented in previous studies (Sun et al., 2015; Zhang et al., 2019). The number concentration of condensation nuclei (CN) at each size was measured by a scanning mobility particle sizer, which is equipped with a differential mobility analyzer (DMA; model 3081, TSI) and a condensation particle counter (CPC; model 3772, TSI). Then the mono-dispersed particles were introduced into a Droplet Measurement Technologies CCN counter (CCNc, DMT; Lance et al., 2006) to measure CCN number concentration. A hygroscopic tandem differential mobility analyzer (HTDMA) system was used to measure the hygroscopic growth factor (Gf) (Tan er al., 2013). Here four diameters of 40, 80, 110, 150, and 200 nm are selected in the campaign. Gf is defined as the ratio of the mobility diameter at the given RH to the dry diameter (Petters and Kreidenweis, 2007). The nonrefractory submicron aerosol chemical composition was measured by an Aerosol Chemical Speciation Monitor (ACSM; Sun et al., 2015), including sulfate, nitrate, ammonium, chloride, and organics. Two factors, including a non-hygroscopic primary organic aerosol (POA) and hygroscopic secondary organic aerosol (SOA) were classified by using positive matrix factorization (PMF) with PMF algorithm (v4.2) method (Paatero and Tapper, 1994) and followed the procedures reported in Ulbrich et al., 2009. The refractory black carbon mass loading was measured by an aethalometer (model AE33, Magee Scientific Corporation). Both the nonrefractory materials and BC mass concentration were

https://doi.org/10.5194/acp-2022-542
Preprint. Discussion started: 2 September 2022


Atmospheric Chemistry and Physics Discussions

measured with diameters < 1.0 μm. The detailed description of the instrument operation and data process have been described in details elsewhere (Ren et al., 2018; Xu et al., 2019; Zhang et al., 2019; Fan et al., 2020).

2.2 Retrieving the mixing state and density of BC

The Gf probability distribution function (Gf-PDF) for a specified diameter can be retrieved firstly based on the TDMAinv algorithm (Gysel et al., 2009). The κ-PDF can be further calculated based on the Gf-PDF (Fan et al., 2020). Size-resolved κ is derived using κ-Köhler theory based on hygroscopic growth factor (Gf) (Petters and Kreidenweis, 2007),

$$\kappa_{gf} = (\mathrm{Gf}^3 - 1) \cdot \left[\frac{1}{\mathrm{RH}} \exp\left(\frac{4\sigma_{s/a} M_w}{RT\rho_w \mathrm{D_d Gf}}\right) - 1\right] \quad (1)$$

where Gf is hygroscopic growth factor, RH is the relative humidity in the HTDMA (90 %), D_d is the dry diameter, $\sigma_{s/a}$ is assumed to be the surface tension of pure water, R is the universal gas constant, T is the temperature, M_w and ρ_w is the molecular mass, and the density of water, respectively.

The κ-PDF patterns of particles in different sizes always present two modes: nearly hydrophobic (NH) mode with $\kappa_{gf} \leq 0.1$ and more hygroscopic (MH) mode with $\kappa_{gf} > 0.1$ (Fig. S1). Firstly, based on the κ-PDF patterns, the number fraction (NF) of the total nearly hydrophobic group with the boundary of [0, 0.1] was calculated by using the following equation:

$$NF = \int_0^{0.1} c(\kappa, D_p)\, d\kappa \quad (2)$$

https://doi.org/10.5194/acp-2022-542
Preprint. Discussion started: 2 September 2022


Atmospheric Chemistry and Physics Discussions

Here, the κ-PDF, represented by c (κ, D_p), was normalized as $\int c(\kappa, D_p)\, d\kappa = 1$, where κ can be replaced by κ_{gf}, D_p is the selected electrical mobility diameter in the campaign.

Considering the nearly hydrophobic mode consists of both external mixed POA (Ex-POA or bare POA) and externally mixed BC (Ex-BC). Here, the number fraction of POA in nearly hydrophobic mode ($NF_{NH\text{-}POA}$) was assumed to be 70 % according to the simultaneous measurements (Liu et al., 2021), and the rest 30 % of POA is assumed mixed with the other hygroscopic aerosols. And thus, the number fraction of Ex-BC was calculated using the total number fraction of NH mode minus the number fraction of NH-POA. Then, the number size distribution of the external mixed BC ($n_{Ex\text{-}BC}$ (log D_p)) can be calculated based on the particle number size distribution (PNSD) and the number fraction of the hydrophobic mode of BC ($NF_{Ex\text{-}BC}$) as follows:

$$n_{Ex-BC}(\log Dp) = NF_{Ex-BC} \times n\ (\log Dp) \quad (3)$$

where n (log D_p) is the function of the aerosol number size distribution, D_p is the mobility diameter.

By assuming that the particles are spherical (Rader and McMurry, 1986), the mass size distribution of Ex-BC ($M_{Ex\text{-}BC}$) was obtained as follows:

$$M_{Ex-BC}(\log Dp) = \frac{\pi}{6} {D_p}^3 \rho n_{Ex-BC}(\log Dp) \quad (4)$$

where D_p is the mobility diameter, ρ is the effective density of Ex-BC, and $n_{Ex\text{-}BC}$ (log D_p) is the function of the number size distribution of Ex-BC, respectively. Here we assume that the Ex-BC effective density is 0.40 g cm^{-3} according to previous measurements reported in North China Plain (Peng et al., 2016, 2017; Wu et al., 2019;

https://doi.org/10.5194/acp-2022-542
Preprint. Discussion started: 2 September 2022


Atmospheric Chemistry and Physics Discussions

Liu et al., 2020).

The Ex-BC mass size distributions was modelled as a single log-normal distribution as shown in Fig. S2 (Wu et al., 2017; D. Liu et al., 2019). Thus, the bulk mass concentration of Ex-BC can be calculated from the integration of the mass size distribution:

$$m_{\mathrm{Ex-BC}} = \int_{D_{start}}^{D_{end}} M_{\mathrm{Ex-BC}}(\log\ D_p)\ d\log(D_p) \quad (5)$$

$$m_{\mathrm{In-BC}} = m_{\mathrm{BC}} - m_{\mathrm{Ex-BC}} \quad (6)$$

where D_{start} and D_{end} are the lower and upper size limit, $M_{\mathrm{Ex\text{-}BC}}$ (log D_{p}) is the function of the Ex-BC mass size distribution. We then obtained the bulk mass concentration of internally mixed BC ($m_{\mathrm{In\text{-}BC}}$) by minus $m_{\mathrm{Ex\text{-}BC}}$ from the bulk BC mass concentration measured by AE33 in the equation 6.

For retrieval of the density of BC, the principal idea is to use the measured κ_{gf} to calculate the density of BC based on the Zdanovskii–Stokes–Robinson (ZSR) mixing rule (Stokes and Robinson, 1966; Zdanovskii, 1948) with the chemical composition measured by ACSM (Petters & Kreidenweis, 2007). In the retrieval, several aspects are concerned. First, since the ZSR rule is with an assumption of the aerosol particles are internally mixed, the κ_{gf} value of the more MH mode ($\kappa_{\mathrm{gf\text{-}MH}}$) is thus applied for retrieving the density of internally-mixed BC. Second, since the size distribution of BC number concentration is usually with peaks between 100 and 200 nm (D. Liu et al., 2019; Yu et al., 2020; Zhao et al., 2022), the $\kappa_{\mathrm{gf\text{-}MH}}$ value of particles in accumulation mode, which showed an independence on particle size when the D_{p} >100 nm during the campaign period (Fan et al., 2020), was averaged and applied for the retrieval. In

https://doi.org/10.5194/acp-2022-542
Preprint. Discussion started: 2 September 2022

Atmospheric Chemistry and Physics Discussions

addition, because the inversion including measurements from HTDMA and ACSM, a total mass closure of the measured aerosol particles was conducted between the two techniques by comparing the mass concentration of PM_1 and the results are well consistent (Fig. S3). The density of internally-mixed BC (In-BC), $\rho_{\text{In-BC}}$ is then derived from the following equations:

$$\kappa_{gf-MH} = \kappa_{chem} = \sum_i \varepsilon_i \kappa_i = \frac{v_{inorg}}{v_{total}}\kappa_{inorg} + \frac{v_{SOA}}{v_{total}}\kappa_{SOA} + \frac{v_{In-POA}}{v_{total}}\kappa_{POA} + \frac{v_{In-BC}}{v_{total}}\kappa_{BC} \quad (7)$$

where $\kappa_{\text{gf-MH}}$ is the hygroscopic parameter of the more hygroscopic (MH) mode, κ_{chem} is the hygroscopic parameter of aerosol particles in the mixed composition and can be calculated based on chemical volume fractions by using a simple rule (Petters & Kreidenweis, 2007), κ_{i} is the hygroscopic parameter of each pure composition and ε_{i} is the volume faction of the individual components in the internal-mixed particle. v_{inorg}, v_{SOA} and $v_{\text{In-POA}}$ are the volume of the inorganic, SOA and internally mixed POA species, and can be calculated as follows: $v_{inorg} = \frac{m_{inorg}}{\rho_{inorg}}$, $v_{SOA} = \frac{m_{SOA}}{\rho_{SOA}}$, and $v_{In-POA} = \frac{m_{In-POA}}{\rho_{POA}}$. v_{total} is the total volume of all the species and can be written as $v_{total} = \frac{m_{inorg}}{\rho_{inorg}} + \frac{m_{SOA}}{\rho_{SOA}} + \frac{m_{In-POA}}{\rho_{POA}} + \frac{m_{In-BC}}{\rho_{In-BC}}$. In the equation (7), κ_{BC} and κ_{POA} are assumed to be 0. Then, the $\rho_{\text{In-BC}}$ can be calculated based on its mass concentration and volume as follows:

$$\rho_{In-BC} = \frac{m_{In-BC}}{\left(\frac{\frac{m_{inorg}}{\rho_{inorg}}\kappa_{inorg} + \frac{m_{SOA}}{\rho_{SOA}}\kappa_{SOA}}{\kappa_{gf-MH}} - \frac{m_{inorg}}{\rho_{inorg}} - \frac{m_{SOA}}{\rho_{SOA}} - \frac{m_{In-POA}}{\rho_{POA}}\right)} \quad (8)$$

where, $m_{\text{In-BC}}$ is the mass concentration of internal-mixed BC, m_{inorg} and m_{SOA} are the mass concentrations of the inorganic species and SOA, which are measured by the ACSM. $m_{\text{In-POA}}$ is the mass concentrations of internal-mixed POA and can be calculated by using the total mass concentrations of POA minus the mass fraction of NH-POA. ρ_{inorg}, ρ_{SOA} and ρ_{POA} are the density of the inorganic species, SOA and POA. Here

https://doi.org/10.5194/acp-2022-542
Preprint. Discussion started: 2 September 2022


Atmospheric Chemistry and Physics Discussions

inorganic species were derived by applying a simplified ion pairing scheme (Gysel et al., 2007). Three inorganic salts including NH_4HSO_4, $(NH_4)_2SO_4$, and NH_4NO_3 were applied in our study. The densities for inorganic salts and organics were referred from the articles published (Gysel et al., 2007; Wu et al., 2016). Here the densities for three inorganics are 1.78, 1.79 and 1.72 g cm^{-3}, respectively. And the ρ_{SOA} and ρ_{POA} are assumed as 1.4 and 1.0 g cm^{-3}. The values of κ for each pure component was refereed from Petters & Kreidenweis, 2007 and Gunthe et al., 2009. For the inorganic compounds, the κ values are 0.56 for NH_4HSO_4, 0.48 for $(NH_4)_2SO_4$ and 0.58 for NH_4NO_3. The κ_{SOA} is assumed to be 0.15 according to the field studies in urban areas (Chang et al., 2010; Kawana et al., 2016).

2.3 Uncertainties and limitations

For the retrieval, the assumptions on the values of κ_{SOA}, ρ_{POA}, ρ_{SOA} and $\rho_{Ex\text{-}BC}$ as well as the fraction of primary organic aerosols in non-hygroscopic or hygroscopic mode would add uncertainty in the inferred values of ambient internally-mixed BC density. Therefore, we examined the sensitivities of In-BC density to the variations of these factors, as exhibited in Fig. 1. Within a typical atmospheric observed range of 50-90 % for the $NF_{NH\text{-}POA}$ (Liu et al., 2021), the assumption on $NF_{NH\text{-}POA}$ can lead to relative deviations (uncertainty) of -20 %–+30 % for the retrieved BC density (Fig. 2a).

In addition, unlike inorganics, which the hygroscopicity has been already well-understood (Petters and Kreidenweis, 2007), the hygroscopicity of organic species varies largely due to the complexity in organic aerosol constituents. Therefore, the

https://doi.org/10.5194/acp-2022-542
Preprint. Discussion started: 2 September 2022

Atmospheric Chemistry and Physics Discussions

assumption of the values of κ_{SOA} will add the uncertainty in the calculation of BC density. Previous studies have suggested that the organics has a wide range of κ values ranging from 0.05 to 0.3 (Jimenez et al., 2009; Mei et al., 2013). Thus, the sensitivity test has also been done to examine the effect due to changes in κ_{SOA} on calculating the density of BC (Fig. 1a). The result shows that the assumption of κ_{SOA} value can cause an average relative deviation of -20 %–+10 % in calculating the density of In-BC (Fig. 2b). However, the sensitivity test shows that the impact of both the ρ_{POA} and ρ_{SOA} variations on the BC density estimation is very small or even negligible (Fig. 1b, c). By varying the ρ_{POA} from 0.85 to 1.0 g cm^{-3} and the ρ_{SOA} from 1.2 to 1.4 g cm^{-3} according

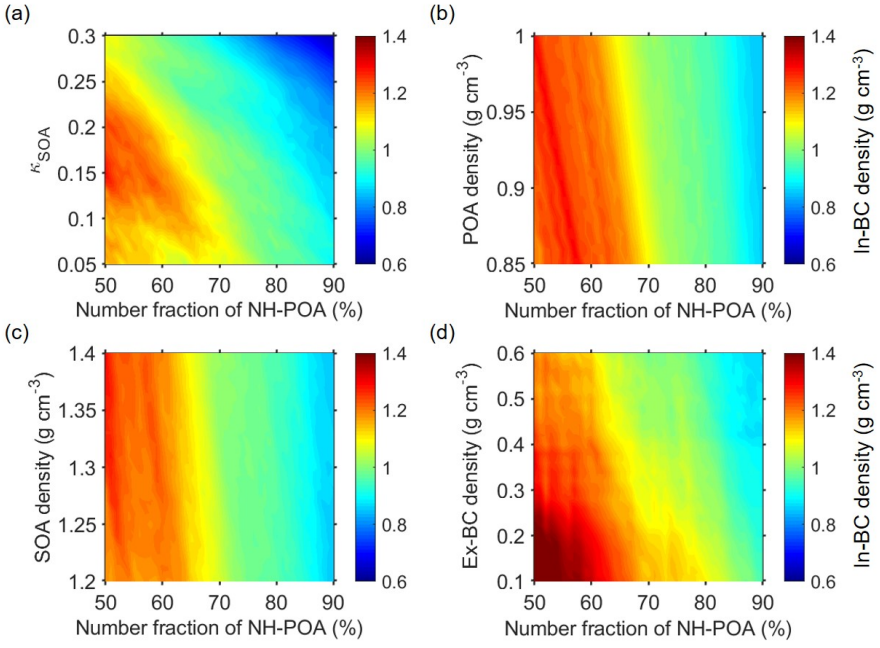

Figure 1. Sensitivities of In-BC density to the variations in the number fraction of nearly hydrophobic (NH) POA and hygroscopic parameter of OA (k_{SOA}) (a), POA density (b), SOA density (c) and the externally-mixed BC density (d).

https://doi.org/10.5194/acp-2022-542
Preprint. Discussion started: 2 September 2022

Atmospheric Chemistry and Physics Discussions

to the literatures (Noureddini et al., 1992; Alfarra et al., 2006; Reyes-Villegas et al., 2018), the retrieval uncertainties in the BC density are within ±10 % and ±5 % respectively (Fig. 2c, d). Similarly, it exhibits that the variations of the $\rho_{Ex\text{-}BC}$ would

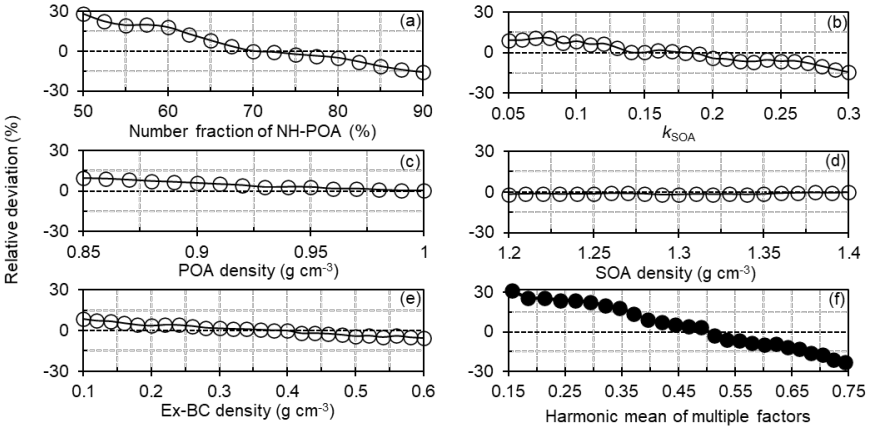

Figure 2. Relative deviations of the number fraction of nearly hydrophobic (NH) POA to the In-BC density (a), the hygroscopic parameter of OA to the In-BC density (b), the POA density to the In-BC density (c), the SOA density to the In-BC density (d), the externally-mixed BC density to In-BC density (e) and the combined deviations based on multiple factors mentioned above (f).

cause an average deviation of ±10 % (Fig. 2e) in retrieved In-BC density when increasing the values of $\rho_{Ex\text{-}BC}$ from 0.10 to 0.60 g cm^{-3}, which represents a typical range of $\rho_{Ex\text{-}BC}$ in ambient atmosphere (Wu et al., 2019; Liu et al., 2020). A combined uncertainty (δ) caused by the multiple factors (δ_i), which is calculated by the equation 9, is -23 %–+31 % as shown in Fig. 2f.

$$\delta = \sqrt{\sum_{i=1}^{n} {\delta_i}^2} \quad (9)$$

Note that, this method fails to retrieve the BC density when organics account for

https://doi.org/10.5194/acp-2022-542
Preprint. Discussion started: 2 September 2022


Atmospheric Chemistry and Physics Discussions

a large fraction (>60 %). This is because that a higher fraction of OA usually corresponds to lower total volume of all the species (Fig. S4), yielding negative values for $v_{\text{In-BC}}$ introduced in equation 10. As a result, 62 % of the data observed during the campaign were valid for calculating the BC density.

$$v_{In-BC} = \frac{v_{inorg}\kappa_{inorg}+v_{SOA}\kappa_{SOA}}{\kappa_{gf-MH}} - v_{inorg} - v_{SOA} - v_{In-POA} \quad (10)$$

Similarly, the bulk density of BC ($\rho_{\text{bulk-BC}}$) is calculated with the same method as that for calculation the $\rho_{\text{In-BC}}$. When calculating the $\rho_{\text{bulk-BC}}$, the bulk κ_{gf} value measured by HTDMA is applied with the assumption of all the aerosol particles are internally mixed.

3 Results and Discussion

3.1 Retrieved mixing state and density of BC: comparison and validation

Figure 3a shows retrieved time series of the mixing state of ambient BC during the campaign. Large temporal variations of the mass fraction of internal and external mixed BC are presented during the observed period at the sites. The temporal changes should be related to the atmosphere aging process or diurnal variations of emissions (D. Liu et al., 2019; Fan et al., 2020). Statistically, the average mass fraction of externally and internally-mixed BC is 21±18 % and 79±18 % respectively, showing that most of the BC particles were aged and internally-mixed with other components. Previous studies at urban sites have shown that the co-existence of the externally mixed BC in the ambient atmosphere (Schwarz et al., 2008; Cheng et al., 2012; Chen et al., 2020) due to continuous combustion processes (e.g., vehicle exhaust and residential sector) (Wang

https://doi.org/10.5194/acp-2022-542
Preprint. Discussion started: 2 September 2022

Atmospheric Chemistry and Physics Discussions

et al., 2017; D. Liu et al., 2019). Our results are basically comparable with both those directly measured or indirectly retrieved previously reported results. For example, Chen et al., 2020 found that the mass fraction of internal mixed BC particles was nearly to be

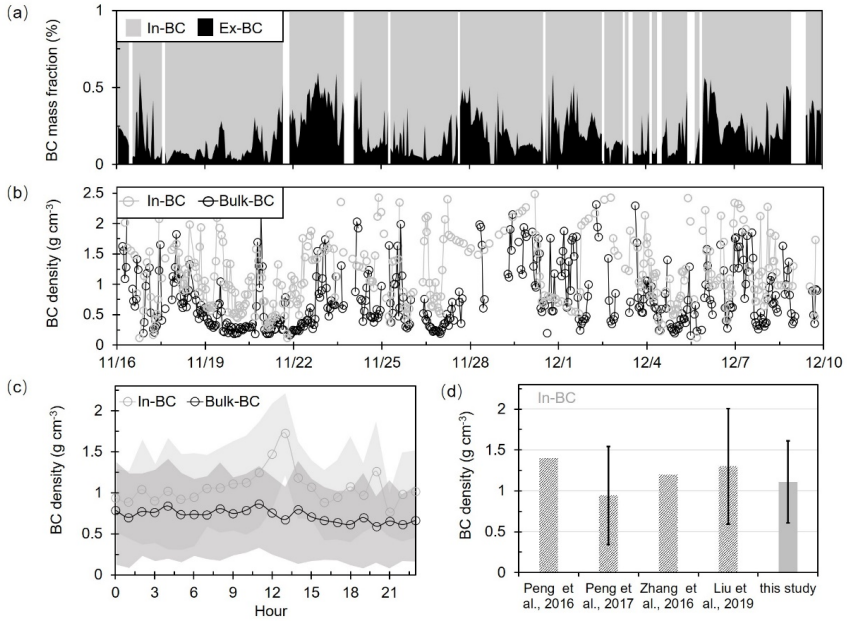

Figure 3. (a) Time series of the mass fraction of the retrieved internal- and external-mixed BC; (b) Time series of the retrieved density of the bulk and internal- mixed BC (In-BC); (c) Diurnal variation of the retrieved density of bulk and In-BC; (d) Comparison of the results of the derived In-BC density in this study with that reported in literatures.

~80–90 % in summer of Beijing based on VTDMA measurements. Liu et al., (2020), using a tandem system with an aerodynamic aerosol classifier and SP2, reported that the mass fraction of internal BC-containing particles would increase with increasing size and reach ~70 % in Beijing. Overall, the mass fraction obtained in our study is

https://doi.org/10.5194/acp-2022-542
Preprint. Discussion started: 2 September 2022


Atmospheric Chemistry and Physics Discussions

comparable with those reported in urban Beijing. Previous studies also displayed that the significant diversity of the BC mixing state among emission conditions and coating process (Shiraiwa et al., 2008; Pan et al., 2017; Zhang et al., 2020). Accordingly, the densities of the bulk and internal mixed BC present apparent fluctuations as shown in Fig. 3b, which is significantly affected by the variations of BC emission sources and its rapid aging process. The density of the In-BC during daytime were generally higher than that at night (Fig. 3c). The elevated BC density during daytime is likely due to that the strong photochemical processes promote the aging of BC particles, which resulted in a conversion from uncompacted structure to compact and regular spherical shapes of BC (Qiao et al., 2018; H. Liu et al., 2019; Zhou et al., 2022). The slightly decreases were observed both in the bulk BC and In-BC density during traffic hours. This is likely associated with the continues emissions (e.g., vehicle exhaust) that lead to more uncoated or uncompacted BC particles in urban regions. The diurnal cycles in BC density are consistent with that measured by a tandem CPMA-SP2-DMA-SP2 (Liu et al., 2020), demonstrating that the new method can derive the density of ambient BC particles reasonably. Averagely, the bulk and internal-mixed BC densities are with campaign averaged values of 0.73±0.46 and 1.11±0.54 g cm^{-3} respectively, which are much less than 1.8 g cm^{-3}, implying that the BC particles is not a void-free spheres in the urban atmosphere. The results of In-BC density are comparable with that observed at the other sites in North China Plain (NCP) as shown in Fig. 3d, illustrating that the BC effective density retrieved by this method is within the range of field measurements. Based on both field measurements (e.g. Lide 1992; Zhang et al., 2016; Wu et al., 2019;

https://doi.org/10.5194/acp-2022-542
Preprint. Discussion started: 2 September 2022

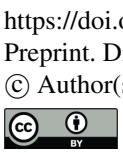

Atmospheric Chemistry and Physics Discussions

322 H. Liu et al., 2019) and laboratory studies (e.g. Mcmurry et al., 2002; Park et al., 2003,
323 2004; Olfert et al., 2007; Kiselev et al., 2010; Gysel et al., 2011, 2012), the BC density
324 from diverse combustion sources or representing different aging degree has been

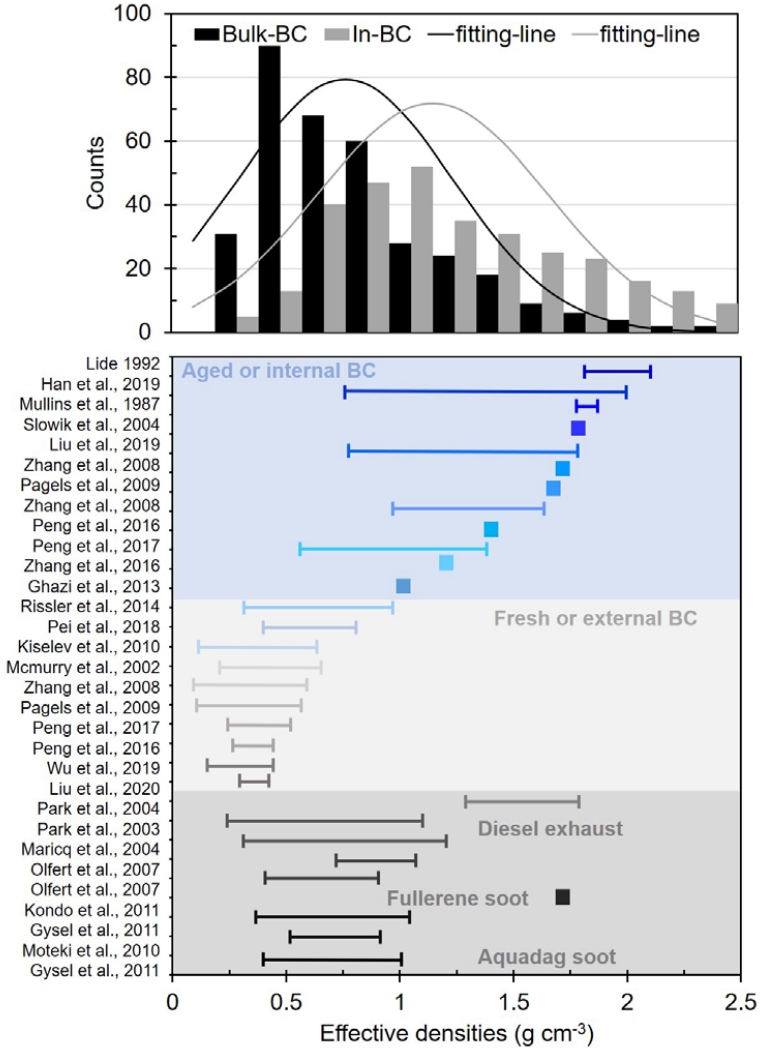

325

326 **Figure 4.** The probability distribution function (PDF) of the retrieved density of bulk
327 and In-BC and the measured density distribution spectrum of BC from different sources
328 reported in literatures.

https://doi.org/10.5194/acp-2022-542
Preprint. Discussion started: 2 September 2022


Atmospheric Chemistry and Physics Discussions

obtained and ranges widely from 0.14 to 2.1 g cm^{-3}, as has been summarized and shown in Fig. 4. Mean probability distribution function (PDF) of the density of bulk and In-BC retrieved by this study are also presented in Fig. 4. It shows that the retrieved density of bulk BC exhibits a dominant mode with peak value of 0.70 g cm^{-3}, which is situated between the typical density range of those externally-mixed and internally-mixed BC measured previously. For the In-BC, the PDF is with a peak value at 1.10 g cm^{-3}, but ranges widely from ~0.5 to 2.4 g cm^{-3}, which indicates various morphologies, different aging degree and compositions of ambient BC particles due to the complex impact of multiple local sources and aging processes during the observed period in urban Beijing. Overall, the retrieved values for In-BC fall within the range of typical internal mixing BC reported in the literatures, verifying the reliability of our inversion results.

3.2 Sensitivity of predicted N_{CCN} to changes of BC density

It has been studied that an inappropriate use of the density value of BC particles will result in large bias in estimating κ of ambient aerosol particles with the ZSR mixing rule (Fan et al., 2020), as would further lead to uncertainties in prediction of N_{CCN} and relevant climate effects. Considering the large variation range of BC density during the campaign, which is closely associated with its morphology or degree of its aging, we further examine the sensitivity of critical supersaturation (S_c), critical diameter (D_{cut}) and predicted N_{CCN} to variations of BC density (Fig. 5). Here, we use the critical diameter and particle number size distribution to calculate N_{CCN}. The method to derive the critical diameter is based on Köhler theory and ZSR rule. Three closure studies were

https://doi.org/10.5194/acp-2022-542
Preprint. Discussion started: 2 September 2022

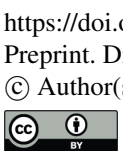

Atmospheric Chemistry and Physics Discussions

used to evaluate the effect of BC density and mixing state on prediction of CCN number concentrations. The detailed calculation methods are presented in the supporting information (SI: Methods) or referenced from Ren et al., 2018.

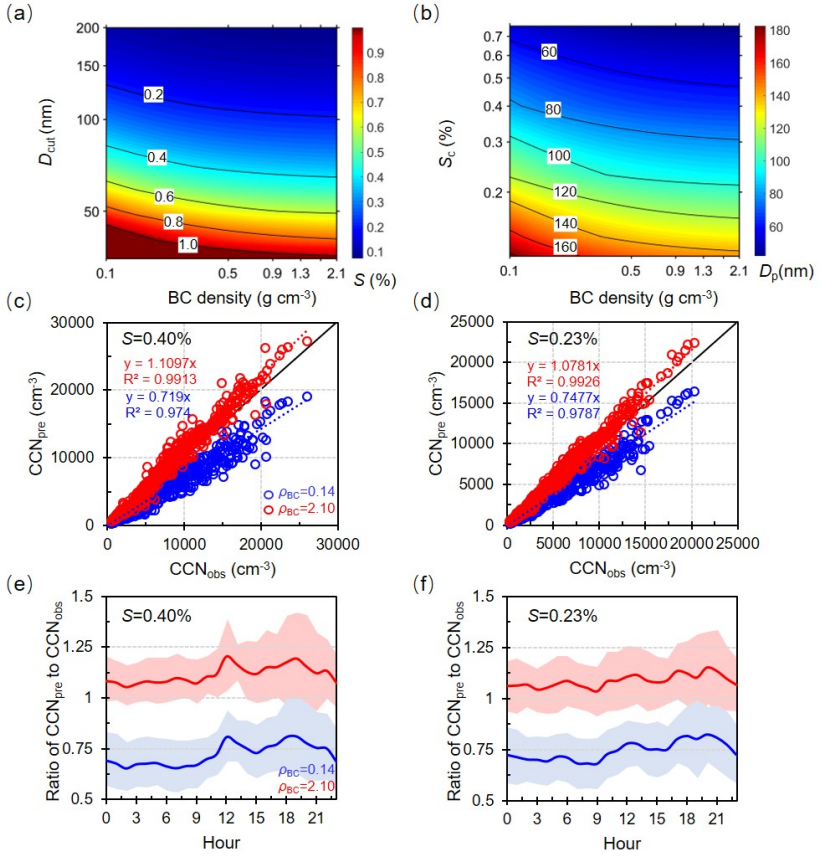

Figure 5. Sensitivity of critical supersaturation (S_c) (a) and diameter (D_{cut}) (b) to the variations in BC density; Predicted N_{CCN} as a function of measured N_{CCN} by varying the density from 0.14 to 2.1 g cm^{-3} at S=0.40 % (c) and S=0.23 % (d), the black solid line is the 1:1 line; Diurnal variations in the ratio of predicted-to-measured N_{CCN} at S=0.40 % (e) and S=0.23 % (f).

The results show that, by varying the value of density from 0.14 to 2.1 g cm^{-3} that

https://doi.org/10.5194/acp-2022-542
Preprint. Discussion started: 2 September 2022


Atmospheric Chemistry and Physics Discussions

represents the lower and upper limit of BC density in the atmosphere), the D_{cut} reduces apparently at a given supersaturation (S) (Fig. 5a), or similarly, the S_c decreases rapidly for a given particle size (Fig. 5b). The results show that the changes of the D_{cut} and S_c are more sensitive when the BC density is below 1.0 g cm^{-3}. And the effects on the D_{cut} and S_c both gradually weakened with the increase of BC density. This shows that it is critical to apply more accurate BC density for the aerosol particles with low aging degree in predicting CCN and its climate effect. Accordingly, the ratios of predicted-to-measured N_{CCN} ranged from 0.72 to 1.11 by varying the BC density from 0.14 to 2.1 g cm^{-3} at the typical S of 0.2 % and 0.4 % (Fig. 5c, 5d), showing an estimation uncertainty of -28 %–11 % in N_{CCN} prediction.

The diurnal variations in the ratio of predicted-to-measured N_{CCN} at S=0.40 % and 0.23 % are shown to examine the response of the BC density on N_{CCN} prediction at different time periods (Fig. 5e, 5f). By applying the lower limit of density value of 0.14 g cm^{-3}, the prediction is much worse compared to the use of the density of 2.1 g cm^{-3} at nighttime (00:00-06:00 LT), when the latter is much closer to the real density of ambient BC (Fig. 3c). The prediction is improved substantially by applying the value of 0.14 g cm^{-3} during evening rush hours (18:00-20:00 LT), during which the ambient BC particles is more externally-mixed with smaller densities (Fig. 3c). And now, the prediction becomes worse by applying the value of 2.1 g cm^{-3}, and an obvious overestimation by up to ~40 % is shown. The results further illustrate that it is critical to account for the real-time mixing state and density of BC particles in N_{CCN} prediction, in particular in those regions with heavy traffic and residential coal emissions.

https://doi.org/10.5194/acp-2022-542
Preprint. Discussion started: 2 September 2022

Atmospheric Chemistry and Physics Discussions

382 **3.3 Using the real-time variations of BC density and mixing state to predict N_{CCN}**

383 Figure 6 exhibits the comparisons between predicted and measured N_{CCN} at S of
384 0.2 % and 0.4 % by accounting for the retrieved real-time variations of BC density and
385 mixing state. It shows that the N_{CCN} can be well predicted with a slope of 0.98 and 0.97
386 at S of 0.2 % and 0.4 % respectively (Fig. 6a, 6b), only presenting a slight deviation.
387 The slight underestimation is primarily due to an underestimation of the density for the
388 externally mixed BC caused by the retrieved method, especially during noontime (Fig.
389 6c and 6d).

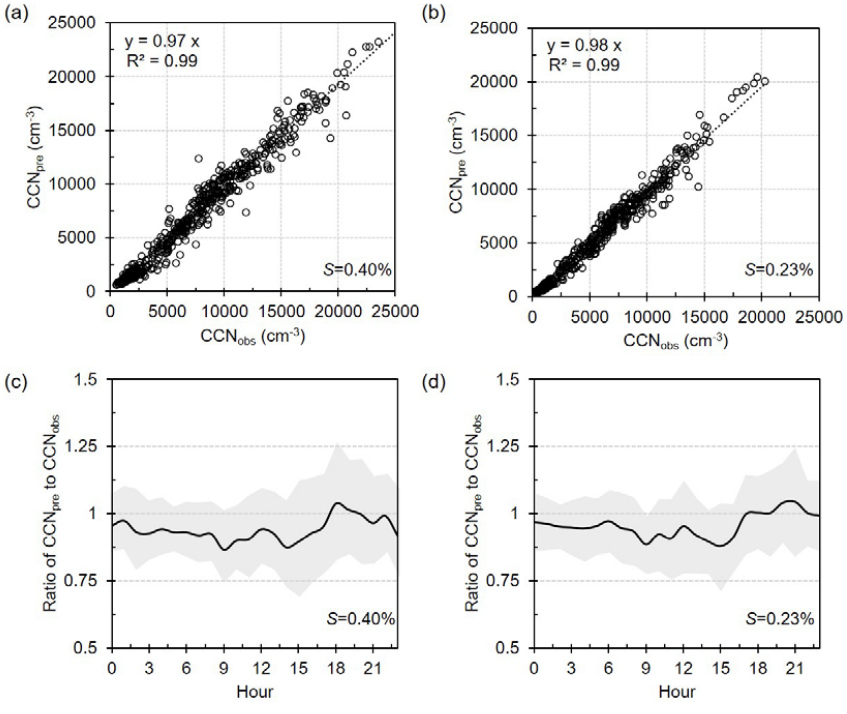

390

391 **Figure 6.** Prediction CCN number concentration by using the mixing state and In-BC
392 density derived from HTDMAs at S=0.40 % (a) and S=0.23 % (b). Diurnal variations
393 in the ratio of predicted-to-measured N_{CCN} at S=0.40 % (c) and S=0.23 % (d).

https://doi.org/10.5194/acp-2022-542
Preprint. Discussion started: 2 September 2022


Atmospheric Chemistry and Physics Discussions

394 The diurnal variations in the ratio of predicted-to-measured N_{CCN} shows the N_{CCN}
395 can be underestimated by up to 20 % at S=0.4 % during those periods. While, a slightly
396 overrated during the evening traffic hours and nighttime may be due to the
397 underestimation of the number fraction of Ex-BC. Overall, the dependence of the CCN
398 prediction on S is due to the size dependence of κ and mixing state (Zhang et al., 2017;
399 Liu et al., 2020; Xu et al., 2021). The better closure at S=0.2 % is because that the bulk
400 κ of particles is closer to that the critical diameter corresponding to S=0.2 %, with D_p
401 of 100-150 nm. Similarly, the effect on CCN prediction induced by the bulk mixing
402 state would be more critical for smaller particles, corresponding to the critical diameter
403 at high S.

404 Overall, when considering the effective density of BC relevant to its mixing state,
405 the CCN closure achieves. Previous studies have shown that the fresh emitted BC
406 particles may convert from fractal-like aggregates to a compact structure and its density
407 would increase with the aging process (Pagels et al., 2009; Rissler et al., 2014; Peng et
408 al., 2016; H. Liu et al., 2019; Zhang et al., 2020, 2022), but the actual density of In-BC
409 may be lower than 1.8 g cm^{-3} in the ambient atmosphere according to this study.
410 Therefore, the currently applied value represents a density of the void-free structure of
411 BC particles may cause an overestimation in CCN prediction.

412 4 Conclusions

413 The mixing state and effective density of BC changed through heterogenous
414 chemistry process and thus would causes uncertainty in evaluating its CCN activity. In

https://doi.org/10.5194/acp-2022-542
Preprint. Discussion started: 2 September 2022


Atmospheric Chemistry and Physics Discussions

this study, we develop a new method to retrieve the mixing state and effective density of ambient BC using field measurements and the Köhler theory. The uncertainty of the new retrieval method was evaluated within ±30 %, which is primarily caused by assumptions of the κ_{SOA} and the fraction of primary organic aerosols in non-hygroscopic or hygroscopic mode. The retrieved results show that most of the BC particles were aged and internally-mixed with other components, with mean mass fraction of 79±18 %. Averagely, the retrieved densities of the bulk and internal mixed BC are 0.73±0.46 and 1.11±0.54 g cm^{-3} respectively, but ranges widely from ~0.1 to 2.4 g cm^{-3}, indicating various morphologies, different aging degree and compositions of ambient BC particles due to the complex impact of multiple local sources and aging processes during the observed period. The retrieved results are basically comparable with the previous observations in North China Plain.

Further examination shows the N_{CCN} prediction is with uncertainties of -28 %–11 % at the typical S of 0.2 % and 0.4 % by varying the BC density from 0.14 to 2.1 g cm^{-3} that represents the lower and upper limit of ambient BC particles. Moreover, the prediction is found more sensitive to the variability of BC density when it is <1.0 g cm^{-3}, suggesting a great significance to account for the effect of BC density for the aerosol particles with low aging degree when evaluating the climate effect. The CCN closure achieves when introducing the retrieved real-time BC density relevant to its mixing state. This work provides a unique way of utilizing field observations to infer ambient BC density and highlights the currently assumption of a void-free structure of BC particles in models would cause large uncertainties in CCN prediction and in the

https://doi.org/10.5194/acp-2022-542
Preprint. Discussion started: 2 September 2022


Atmospheric Chemistry and Physics Discussions

437 relevant climate effect evaluation.

438 Data availability.

439 All data needed to evaluate the conclusions in the paper are present in the paper and/or
440 the Supplement. All data used in the study are also available from the corresponding
441 author upon request (zhangfang2021@hit.edu.cn).

442 Author contributions.

443 FZ and JR conceived the conceptual development of the manuscript. JR directed and
444 performed of the experiments with JL, LC, and FZ. JR conducted the data analysis and
445 wrote the draft of the manuscript. All authors edited and commented on the various
446 sections of the manuscript.

447 Acknowledgments.

448 This work was funded by the National Natural Science Foundation of China (NSFC)
449 research project (41975174, 41675141). We thank all participants in the field campaigns
450 for their tireless work and cooperation. We also thank Dr. Yele Sun and his group for
451 providing the data of nonrefractory submicron aerosol chemical composition.

452 Competing interests.

453 The contact author has declared that neither they nor their co-authors have any

https://doi.org/10.5194/acp-2022-542
Preprint. Discussion started: 2 September 2022

competing interests.

References

Alfarra, M. R., Paulsen, D., Gysel, M., Garforth, A. A., Dommen, J., Prévôt, A. S. H., Worsnop, D. R., Baltensperger, U., and Coe, H.: A mass spectrometric study of secondary organic aerosols formed from the photooxidation of anthropogenic and biogenic precursors in a reaction chamber, Atmos. Chem. Phys., 6, 5279– 5293, https://doi:10.5194/acp-6-5279-2006, 2006.

Bond, T. C., Doherty, S. J., Fahey, D., Forster, P., Berntsen, T., DeAngelo, B., Flanner, M., Ghan, S., Kärcher, B., and Koch, D.: Bounding the role of black carbon in the climate system: A scientific assessment, J. Geophys. Res.-Atmos., 118(11), 5380–5552, https://doi.org/10.1002/jgrd.50171, 2013

Clarke, A.D., Shinozuka, Y., Kapustin, V.N., Howell, S., Huebert, B., Doherty, S., Anderson, T., Covert, D., Anderson, J., Hua, X., Moore II, K.G., McNaughton, C., Carmichael, G., Weber, R.: Size distributions and mixtures of dust and black carbon aerosol in Asian outflow: physiochemistry and optical properties, J. Geophys. Res.-Atmos., 109, D15S09, https://doi.org/10.1029/2003JD004378, 2004.

Cheng, Y. F., Su, H., Rose, D., Gunthe, S. S., Berghof, M., Wehner, B., Achtert, P., Nowak, A., Takegawa, N., Kondo, Y., Shiraiwa, M., Gong, Y. G., Shao, M., Hu, M., Zhu, T., Zhang, Y. H., Carmichael, G. R., Wiedensohler, A., Andreae, M. O., and Pöschl, U.: Size-resolved measurement of the mixing state of soot in the megacity Beijing, China: diurnal cycle, aging and parameterization, Atmos. Chem. Phys., 12, 4477–4491, https://doi.org/10.5194/acp-12-4477-2012, 2012.

Chen, L., F. Zhang, P. Yan, X. Wang, L. Sun, Y. Li, X. Zhang, Y. Sun, and Z. Li.: The large proportion of black carbon (BC)-containing aerosols in the urban atmosphere, Environ. Pollut., 263, 114507, https://doi.org/10.1016/j.envpol.2020.114507, 2020.

Chang, R. Y.-W., Slowik, J. G., Shantz, N. C., Vlasenko, A., Liggio, J., Sjostedt, S. J., Leaitch, W. R., and Abbatt, J. P. D.: The hygroscopicity parameter (κ) of ambient organic aerosol at a field site subject to biogenic and anthropogenic influences: relationship to degree of aerosol oxidation, Atmos. Chem. Phys., 10, 5047–5064, https://doi:10.5194/acp-10-5047-2010, 2010.

Dameto de España, C., Wonaschütz, A., Steiner, G., Rosati, B., Demattio, A., Schuh, H., and Hitzenberger, R.: Long-term quantitative field study of New Particle Formation (NPF) events as a source of Cloud Condensation Nuclei (CCN) in the urban background of Vienna, Atmos. Environ., 164, 289–298, https://doi.org/10.1016/j.atmosenv.2017.06.001, 2017.

Flanner, M. G., Zender, C. S., Randerson, J. T., and Rasch, P. J.: Present-day climate forcing and response from black carbon in snow, J. Geophys. Res.-Atmos., 112, D11202, https://doi.org/10.1029/2006JD008003, 2007.

Fan, X., Liu, J., Zhang, F., Chen, L., Conllins, D., Xu, W., Jin, X., Ren, J., Wang, Y.,Wu, H., Li, S., Sun, Y., Li, Z.: Contrasting size-resolved hygroscopicity of fine particles

https://doi.org/10.5194/acp-2022-542
Preprint. Discussion started: 2 September 2022


Atmospheric Chemistry and Physics Discussions

derived by HTDMA and HR-ToF-AMS measurements between summer and winter in Beijing: the impacts of aerosol aging and local emissions, Atmos. Chem. Phys. 20, 915-929, https://doi.org/10.5194/acp-20-915-2020, 2020.

Gysel, M., McFiggans, G. B., and Coe, H.: Inversion of tandem differential mobility analyser (TDMA) measurements, J. Aerosol Sci., 40, 134–151, https://doi.org/10.1016/j.jaerosci.2008.07.013, 2009.

Gysel, M., Crosier, J., Topping, D. O., Whitehead, J. D., Bower, K. N., Cubison, M. J., Williams, P. I., Flynn, M. J., McFiggans, G. B., and Coe, H.: Closure study between chemical composition and hygroscopic growth of aerosol particles during TORCH2, Atmos. Chem. Phys., 7, 6131–6144, https://doi.org/10.5194/acp-7-6131-2007, 2007.

Gunthe, S. S., King, S. M., Rose, D., Chen, Q., Roldin, P., Farmer, D. K., Jimenez, J. L., Artaxo, P., Andreae, M. O., Martin, S. T., and Pöschl, U.: Cloud condensation nuclei in pristine tropical rainforest air of Amazonia: size resolved measurements and modeling of atmospheric aerosol composition and CCN activity, Atmos. Chem. Phys., 9, 7551–7575, https://doi.org/10.5194/acp-9-7551-2009, 2009.

Gysel, M., Laborde, M., Olfert, J. S., Subramanian, R., & Gröhn, A. J.: Effective density of aquadag and fullerene soot black carbon reference materials used for SP2 calibration, Atmos. Meas. Tech., 4(12), 4937–4955, https://doi.org/10.5194/amt-4-2851-2011, 2011.

Gysel, M., Laborde, M., Mensah, A. A., Corbin, J. C., Keller, A., Kim, J., et al.: Technical note: The single particle soot photometer fails to reliably detect PALAS soot nanoparticles, Atmos. Meas. Tech., 5(12), 3099–3107, https://doi.org/10.5194/amt-5-3099-2012, 2012.

Jimenez, J. L., Canagaratna, M. R., Donahue, N. M., Prevot, A. S. H., Zhang, Q., Kroll, J. H., DeCarlo, P. F., Allan, J. D., Coe, H., Ng, N. L., Aiken, A. C., Docherty, K. S., Ulbrich, I. M., Grieshop, A. P., Robinson, A. L., Duplissy, J., Smith, J. D., Wilson, K. R., Lanz, V. A., Hueglin, C., Sun, Y. L., Tian, J., Laaksonen, A., Raatikainen, T., Rautiainen, J., Vaattovaara, P., Ehn, M., Kulmala, M., Tomlinson, J. M., Collins, D. R., Cubison, M. J., Dunlea, E. J., Huffman, J. A., Onasch, T. B., Alfarra, M. R., Williams, P. I., Bower, K., Kondo, Y., Schneider, J., Drewnick, F., Borrmann, S., Weimer, S., Demerjian, K., Salcedo, D., Cottrell, L., Griffin, R., Takami, A., Miyoshi, T., Hatakeyama, S., Shimono, A., Sun, J. Y., Zhang, Y. M., Dzepina, K., Kimmel, J. R., Sueper, D., Jayne, J. T., Herndon, S. C., Trimborn, A. M., Williams, L. R., Wood, E. C., Middlebrook, A. M., Kolb, C. E., Baltensperger, U., and Worsnop, D. R.: Evolution of Organic Aerosols in the Atmosphere, Science., 326, 1525–1529, https://doi.org/10.1126/science.1180353, 2009.

Kiselev, A., Wennrich, C., Stratmann, F., Wex, H., Henning, S., Mentel, T.F., Kiendler-Scharr, A., Schneider, J., Walter, S., Lieberwirth, I.: Morphological characterization of soot aerosol particles during LACIS Experiment in November (LExNo), J. Geophys. Res. -Atmos., 115, D11204. https://doi.org/10.1029/2009jd012635, 2010.

Khalizov, A. F., Zhang, R., Zhang, D., Xue, H., Pagels, J., and McMurry, P. H.: Formation of highly hygroscopic soot aerosols upon internal mixing with sulfuric acid vapor, J. Geophys. Res.-Atmos., 114, D05208, https://doi.org/10.1029/2008jd010595, 2009.

https://doi.org/10.5194/acp-2022-542
Preprint. Discussion started: 2 September 2022

Atmospheric Chemistry and Physics Discussions

Kawana, K., Nakayama, T., and Mochida, M.: Hygroscopicity and CCN activity of atmospheric aerosol particles and their relation to organics: Characteristics of urban aerosols in Nagoya, Japan, J. Geophys. Res.-Atmos., 121, 4100–4121, https://doi.org/10.1002/2015JD023213, 2016.

Li, M., Zhang, Q., Kurokawa, J.-I., Woo, J.-H., He, K., Lu, Z., Ohara, T., Song, Y., Streets, D. G., Carmichael, G. R., Cheng, Y., Hong, C., Huo, H., Jiang, X., Kang, S., Liu, F., Su, H., and Zheng, B.: MIX: a mosaic Asian anthropogenic emission inventory under the international collaboration framework of the MICS-Asia and HTAP, Atmos. Chem. Phys., 17, 935–963, https://doi.org/10.5194/acp-17-935-2017, 2017.

Liu, D., Joshi, R., Wang, J., Yu, C., Allan, J. D., Coe, H., Flynn, M. J., Xie, C., Lee, J., Squires, F., Kotthaus, S., Grimmond, S., Ge, X., Sun, Y., and Fu, P.: Contrasting physical properties of black carbon in urban Beijing between winter and summer, Atmos. Chem. Phys., 19, 6749–6769, https://doi.org/10.5194/acp-19-6749-2019, 2019.

Liu, D., Allan, J., Whitehead, J., Young, D., Flynn, M., Coe, H., McFiggans, G., Fleming, Z. L., and Bandy, B.: Ambient black carbon particle hygroscopic properties controlled by mixing state and composition, Atmos. Chem. Phys., *13*, 2015–2029, https://doi.org/10.5194/acp-13-2015-2013, 2013.

Liu, H., Pan, X.L., Wu, Y., Wang, D.W., Tian, Y., Liu, X.Y., et al.: Effective densities of soot particles and their relationships with the mixing state at an urban site in the Beijing megacity in the winter of 2018, Atmos. Chem. Phys. 19, 14791–14804, https://doi.org/10.5194/acp-19-14791-2019, 2019.

Lide, D. R. (ed.). CRC Handbook of Chemistry and Physics. CRC Press: Ann Arbor, MI. (1992).

Lance, S., Medina, J., Smith, J., and Nenes, A.: Mapping the operation of the DMT continuous flow CCN counter, Aerosol Sci. Tech., 40, 242–254, https://doi.org/10.1080/02786820500543290, 2006.

Liu, H., Pan, X., Liu, D., Liu, X., Chen, X., Tian, Y., Sun, Y., Fu, P., and Wang, Z.: Mixing characteristics of refractory black carbon aerosols at an urban site in Beijing, Atmos. Chem. Phys., 20, 5771–5785, https://doi.org/10.5194/acp-20-5771-2020, 2020.

Liu, L, Zhang, J, Zhang, Y, Wang, Y, Xu, L, Yuan, Q, et al.: Persistent residential burning-related primary organic particles during wintertime hazes in North China: insights into their aging and optical changes, Atmos. Chem. Phys. *21*, 2251–2265, https://doi.org/10.5194/acp-21-2251-2021, 2021.

McMurry, H. Peter, Wang Xin, Park Kihong & Ehara Kensei.: The Relationship between Mass and Mobility for Atmospheric Particles: A New Technique for Measuring Particle Density, Aerosol Sci. Technol., 36:2, 227-238, https://doi.10.1080/027868202753504083, 2002.

Massoli, P., Onasch, T.B., Cappa, C.D., Nuamaan, I., Hakala, J., Hayden, K., Li, S.M., Sueper, D.T., Bates, T.S., Quinn, P.K., Jayne, J.T., Worsnop, D.R.: Characterization of black carbon-containing particles from soot particle aerosol mass spectrometer measurements on the R/V Atlantis during CalNex 2010, J. Geophys. Res.- Atmos.,

https://doi.org/10.5194/acp-2022-542
Preprint. Discussion started: 2 September 2022

120, 2575-2593, https://doi.org/10.1002/2014JD022834, 2015.

Mei, F., Setyan, A., Zhang, Q., and Wang, J.: CCN activity of organic aerosols observed downwind of urban emissions during CARES, Atmos. Chem. Phys., 13, 12155–12169, https://doi.org/10.5194/acp-13-12155-2013, 2013.

Noureddini, H., Teoh, B. C., Davis Clements, L.: Densities of vegetable oils and fatty acids, J. Am. Oil Chem. Soc., 69 (12), 1184−1188, 1992.

Olfert, J. S., Symonds, J. P. R., and Collings, N.: The effective density and fractal dimension of particles emitted from a light-duty diesel vehicle with a diesel oxidation catalyst, J. Aerosol Sci., 38, 69–82, https://doi.org/10.1016/j.jaerosci.2006.10.002, 2007.

Park, K., Kittelson, D. B., and McMurry, P. H.: Structural properties of diesel exhaust particles measured by transmission electron microscopy (TEM): Relationships to particle mass and mobility, Aerosol Sci. Technol., 38, 881–889, https://doi.org/10.1080/027868290505189, 2004.

Pagels, J., Khalizov, A.F., McMurry, P.H. and Zhang, R.Y.: Processing of soot by controlled sulphuric acid and water condensation-mass and mobility relationship, Aerosol Sci. Technol., 43, 629–640, https://doi.org/10.1080/02786820902810685, 2009.

Peng, J. F., Hu, M., Guo, S., Du, Z. F., Zheng, J., Shang, D. J., Zamora, M., Zeng, L. M., Shao, M., Wu, Y. S., Zheng, J., Wang, Y., Glen, C., Collins, D., Molina, M., and Zhang, R. Y.: Markedly enhanced absorption, and direct radiative forcing of black carbon under polluted urban environments, P. Natl. Acad. Sci. USA, 113(16), 4266–4271, https://doi.org/10.1073/pnas.1602310113, 2016.

Petters, M. D. and Kreidenweis, S. M.: A single parameter representation of hygroscopic growth and cloud condensation nucleus activity, Atmos. Chem. Phys., 7, 1961–1971, https://doi.org/10.5194/acp-7-1961-2007, 2007.

Paatero, P. and Tapper, U.: Positive matrix factorization: A nonnegative factormodel with optimal utilization of error estimates of data values, Environmetrics, 5, 111–126, 1994.

Peng, J. F., Hu, M., Guo, S., Du, Z. F., Zheng, J., M., Zeng, L. M., Shao, M., Wu, Y. S., Collins, D., Molina, M., and Zhang, R. Y.: Ageing and hygroscopicity variation of black carbon particles in Beijing measured by a quasi-atmospheric aerosol evolution study (QUALITY) chamber, Atmos. Chem. Phys., 17(17), 10333-10348, https://doi.org/10.5194/acp-17-10333-2017, 2017.

Pan, X.L., Kanaya, Y., Taketani, F., Miyakawa, T., Inomata, S., Komazaki, Y., et al.: Emission characteristics of refractory black carbon aerosols from fresh biomass burning: a perspective from laboratory experiments, Atmos. Chem. Phys., 17(21), 13001–13016, https://doi.org/10.5194/acp-17-13001-2017, 2017.

Park, K., Cao, F., Kittelson, D. B., & McMurry, P. H.: Relationship between particle mass and mobility for diesel exhaust particles, Environ. Sci. Tehnol., 37, 577–583, https://doi.org/10.1021/es025960v, 2003.

Qiao, K., Wu, Z., Pei, X., Liu, Q., Shang, D., Zheng, J., Du, Z., Zhu,W.,Wu, Y., Lou, S., Guo, S., Chan, C.K., Pathak, R.K., Hallquist, M., Hu, M.: Size-resolved effective

https://doi.org/10.5194/acp-2022-542
Preprint. Discussion started: 2 September 2022

density of submicron particles during summertime in the rural atmosphere of Beijing. China, J. Environ. Sci. (China) 73, 69–77. https://doi.org/10.1016/j.jes.2018.01.012, 2018.

Rissler, J., Nordin, E. Z., Eriksson, A. C., Nilsson, P. T., Frosch, M., Sporre, M. K., Wierzbicka, A., Svenningsson, B., Londahl, J., Messing, M. E., Sjogren, S., Hemmingsen, J. G., Loft, S., Pagels, J. H., and Swietlicki, E.: Effective Density and Mixing State of Aerosol Particles in a Near-Traffic Urban Environment, Environ. Sci. Technol., 48, 6300–6308, https://doi.org/10.1021/es5000353, 2014.

Riemer, N., Vogel, H., and Vogel, B.: Soot aging time scales in polluted regions during day and night, Atmos. Chem. Phys., 4, 1885–1893, https://doi.org/10.5194/acp-4-1885-2004, 2004.

Ramanathan, V. and Carmichael, G.: Global and regional climate changes due to black carbon, Nat. Geosci., 36, 221-227, https://doi.org/10.1038/ngeo156, 2008.

Ren, J., Zhang, F., Wang, Y., Collins, D., Fan, X., Jin, X., et al.: Using different assumptions of aerosol mixing state and chemical composition to predict CCN concentrations based on field measurements in urban Beijing, Atmos. Chem. Phys., 18, 6907–6921, https://doi.org/10.5194/acp-18-6907-2018, 2018.

Rader, D.J., McMurry, P.H.: Application of the tandem differential mobility analyzer to studies of droplet growth or evaporation, J. Geophys. Res.- Atmos., 17, 771-787, https://doi.org/10.1016/0021-8502(86)90031-5, 1986.

Reyes-Villegas, E., Bannan, T., Le Breton, M., Mehra, A., Priestley, M., Percival, C., Coe, H., and Allan, J. D.: Online Chemical Characterization of Food-Cooking Organic Aerosols: Implications for Source Apportionment, Environ. Sci. Technol., 52, 5308–5318, https://doi.org/10.1021/acs.est.7b06278, 2018.

Schwarz, J. P., Gao, R. S., Spackman, J. R., Watts, L. A., Thomson, D. S., Fahey, D. W., Ryerson, T. B., Peischl, J., Holloway, J. S., Trainer, M., Frost, G. J., Baynard, T., Lack, D. A., de Gouw, J. A., Warneke, C., and Del Negro, L. A.: Measurement of the mixing state, mass, and optical size of individual black carbon particles in urban and biomass burning emissions, Geophys. Res. Lett., 35, L13810, https://doi.org/10.1029/2008GL033968, 2008.

Stokes, R. and Robinson, R.: Interactions in aqueous nonelectrolyte solutions, I. Solute-solvent equilibria, J. Phys. Chem.-US, 70, 2126–2131, 1966.

Sun, Y., Du, W., Fu, P., Wang, Q., Li, J., Ge, X., Zhang, Q., Zhu, C., Ren, L., Xu, W., Zhao, J., Han, T., Worsnop, D. R., and Wang, Z.: Primary, and secondary aerosols in Beijing in winter: sources, variations, and processes, Atmos. Chem. Phys., 16, 8309–8329, https://doi.org/10.5194/acp-16-8309-2016,2016.

Sun, Y. L., Wang, Z. F., Du, W., Zhang, Q., Wang, Q. Q., Fu, P. Q., Pan, X. L., Li, J., Jayne, J., and Worsnop, D. R.: Long term real-time measurements of aerosol particle composition in Beijing, China: seasonal variations, meteorological effects, and source analysis, Atmos. Chem. Phys., 15, 10149–10165, https://doi.org/10.5194/acp-15-10149-2015, 2015.

Shiraiwa, M., Kondo, Y., Moteki, N., Takegawa, N., Sahu, L., Takami, A., et al.: Radiative impact of mixing state of black carbon aerosol in Asian outflow, J. Geophys. Res.- Atmos., 113, D24210, https://doi.org/ 10.1029/2008JD010546, 2008.

https://doi.org/10.5194/acp-2022-542
Preprint. Discussion started: 2 September 2022

669 Tan, H., Xu, H., Wan, Q., Li, F., Deng, X., Chan, P. W., Xia, D., and Yin, Y.: Design
670 and application of an unattended multifunctional H-TDMA system, J. Atmos. Ocean.
671 Tech., 30, 1136–1148, https://doi.org/10.1175/JTECH-D-12-00129.1, 2013.
672 Ulbrich, I. M., Canagaratna, M. R., Zhang, Q., Worsnop, D. R., and Jimenez, J. L.:
673 Interpretation of organic components from Positive Matrix Factorization of aerosol
674 mass spectrometric data, Atmos. Chem. Phys., 9, 2891–2918,
675 https://doi.org/10.5194/acp-9- 2891-2009, 2009.
676 Wang, Y., Wan, Q., Meng, W., Liao, F., Tan, H., and Zhang, R.: Long-term impacts of
677 aerosols on precipitation and lightning over the Pearl River Delta megacity area in
678 China, Atmos. Chem. Phys., 11, 12421–12436, https://doi.org/10.5194/acp-11-
679 12421-2011, 2011.
680 Wang, Y. Y., Liu, F. S., He, C. L., Bi, L., Cheng, T. H., Wang, Z. L., Zhang, H., Zhang,
681 X. Y., Shi, Z. B., and Li, W. J.: Fractal dimensions and mixing structures of soot
682 particles during atmospheric processing, Environ. Sci. Tech. Lett., 4, 487–493,
683 https://doi.org/10.1021/acs.estlett.7b00418, 2017.
684 Wu, Y. F., Xia, Y. J., Huang, R. J., Deng, Z. Z., Tian, P., Xia, X. G., et al.: A study of the
685 morphology and effective density of externally mixed black carbon aerosols in
686 ambient air using a size-resolved single-particle soot photometer (SP2), Atmos. Meas.
687 Tech., 12, 4347–4359, https://doi.org/10.5194/amt-12-4347-2019, 2019.
688 Wu, Y., Wang, X., Tao, J., Huang, R., Tian, P., Cao, J., Zhang, L., Ho, K.-F., Han, Z.,
689 and Zhang, R.: Size distribution and source of black carbon aerosol in urban Beijing
690 during winter haze episodes, Atmos. Chem. Phys., 17, 7965–7975,
691 https://doi.org/10.5194/acp-17-7965-2017, 2017.
692 Wu, Z. J., Zheng, J., Shang, D. J., Du, Z. F., Wu, Y. S., Zeng, L. M., Wiedensohler, A.,
693 and Hu, M.: Particle hygroscopicity and its link to chemical composition in the urban
694 atmosphere of Beijing, China, during summertime, Atmos. Chem. Phys., 16, 1123–
695 1138, https://doi.org/10.5194/acp-16-1123-2016, 2016.
696 Xue, H., Khalizov, A. F., Wang, L., Zheng, J., and Zhang, R.: Effects of dicarboxylic
697 acid coating on the optical properties of soot, Phys. Chem. Chem. Phys., 11, 7869–
698 7875, https://doi.org/10.1039/b904129j, 2009.
699 Xu, W., Sun, Y., Wang, Q., Zhao, J., Wang, J., Ge, X., et al.: Changes in aerosol
700 chemistry from 2014 to 2016 in winter in beijing: Insights from high-resolution
701 aerosol mass spectrometry, J. Geophys. Res.-Atmos., 124, 1132–1147.
702 https://doi.org/10.1029/2018jd029245, 2019.
703 Xu, W., Fossum, K. N., Ovadnevaite, J., Lin, C., Huang, R.-J., O'Dowd, C., and
704 Ceburnis, D.: The impact of aerosol size-dependent hygroscopicity and mixing state
705 on the cloud condensation nuclei potential over the north-east Atlantic, Atmos. Chem.
706 Phys., 21, 8655–8675, https://doi.org/10.5194/acp-21-8655-2021, 2021.
707 Yuan, T., Li, Z., Zhang, R., and Fan, J.: Increase of cloud droplet size with aerosol
708 optical depth: An observation and modeling study, J. Geophys. Res.-Atmos., 113,
709 D04201, https://doi.org/10.1029/2007JD008632, 2008.
710 Yu, C., Liu, D., Broda, K., Joshi, R., Olfert, J., Sun, Y., Fu, P., Coe, H., Allan, J.D.:
711 Characterising mass-resolved mixing state of black carbon in Beijing using a
712 morphology-independent measurement method, Atmos. Chem. Phys., 20, 3645–

https://doi.org/10.5194/acp-2022-542
Preprint. Discussion started: 2 September 2022

3661. https://doi.org/10.5194/acp-20-3645-2020, 2020.

Zhang, R. Y., Khalizov, A. F., Pagels, J., Zhang, D., Xue, H. X., and McMurry, P. H.: Variability in morphology, hygroscopicity, and optical properties of soot aerosols during atmospheric processing, P. Natl. Acad. Sci. USA, 105, 10291–10296, https://doi.org/10.1073/pnas.0804860105, 2008.

Zhang, Y., Zhang, Q., Cheng, Y., Su, H., Kecorius, S., Wang, Z., Wu, Z., Hu, M., Zhu, T., Wiedensohler, A., and He, K.: Measuring the morphology and density of internally mixed black carbon with SP2 and VTDMA: new insight into the absorption enhancement of black carbon in the atmosphere, Atmos. Meas. Tech., 9, 1833–1843, https://doi.org/10.5194/amt-9-1833-2016, 2016.

Zdanovskii, A.: New methods for calculating solubilities of electrolytes in multicomponent systems, Zh. Fiz. Khim.C, 22, 1475– 1485, 1948.

Zhang, Y., Zhang, Q., Yao, Z., Li, H.: Particle Size and Mixing State of Freshly Emitted Black Carbon from Different Combustion Sources in China, Environ. Sci. Technol., 54(13): p. 7766-7774, https://doi.org/10.1021/acs.est.9b07373, 2020.

Zhang, F., Wang, Y., Peng, J., Ren, J., Collins, D., Zhang, R., et al.: Uncertainty in predicting CCN activity of aged and primary aerosols, J. Geophys. Res.-Atmos., 122(21), 11723–11736, https://doi.org/10.1002/2017jd027058, 2017.

Zhang, F., Ren, J., Fan, T., Chen, L., Xu, W., Sun, Y., et al.: Significantly enhanced aerosol CCN activity and number, J. Geophys. Res.-Atmos., 124, 14102–14113, https://doi.org/10.1029/2019jd031457, 2019.

Zhang, F., Wang, Y., Peng, J., Chen, L., Sun, Y., Duan, L., Ge, X., Li, Y., Zhao, J., Liu, C., Zhang, X., Zhang, G., Pan, Y., Wang, Y., Zhang, A. L., Ji, Y., Wang, G., Hu, M., Molina, M. J., Zhang, R.: An unexpected catalyst dominates formation and radiative forcing of regional haze, P. Natl. Acad. Sci. USA, 117(8), 3960-3966, https://doi.org/10.1073/pnas.1919343117, 2020.

Zhang, F., Peng, J., Chen, L., Collins, D., Li, Y., Jiang, S., Liu, J., Zhang, R.: The effect of Black carbon aging from NO2 oxidation of SO2 on its morphology, optical and hygroscopic properties, Environ. Res., 212, 113238, https://doi.org/10.1016/j.envres.2022.113238, 2022.

Zhou, Y., Ma, N., Wang, Q., Wang, Z., Chen, C., Tao, J., Hong, J., Peng, L., He, Y., Xie, L., Zhu, S., Zhang, Y., Li, G., Xu, W., et al.: Bimodal distribution of size-resolved particle effective density: results from a short campaign in a rural environ ment over the North China Plain, Atmos. Chem. Phys., 22, 2029–2047. https://doi.org/10.5194/acp-22-2029-2022, 2022.

Zhao, G., Tan, T., Hu, S., Du, Z., Shang, D., Wu, Z., Guo, S., Zheng, J., Zhu, W., Li, M., Zeng, L., and Hu, M.: Mixing state of black carbon at different atmospheres in north and southwest China, Atmos. Chem. Phys., 22, 10861–10873, https://doi.org/10.5194/acp-22-10861-2022, 2022.